

# A Novel Structure to Enhance Second Harmonic Generation in Plasmonic Waveguide

Mahmoud Sarani<sup>1</sup>, Alimorad Khajeh zadeh<sup>2</sup>\*, Mehdi Jafari Shabazzadeh<sup>3</sup>

1. PhD student, Department of Electrical Engineering, Kerman Branch, Islamic Azad University, Kerman, Iran.

2. Assistant Professor, Department of Electrical Engineering, Kerman Branch, Islamic Azad University, Kerman, Iran (Corresponding author).

3. Assistant Professor, Department of Electrical Engineering, Kerman Branch, Islamic Azad University, Kerman, Iran.

\* **Corresponding author email address:** alikhajehzadeh@iauk.ac.ir

**Received:** 2024-10-02

**Reviewed:** 2024-11-10

**Revised:** 2025-01-01

**Accepted:** 2025-02-06

**Published:** 2025-06-30

## Abstract

The graphene plasmonic nano-cavity grating is a novel plasmonic structure that has been proven to significantly boost nonlinear optical second-harmonic production. In this article, we discuss how this structure works (SHG). In the suggested structure, metal niobate is positioned such that it is sandwiched between two distinct metals and a thin sheet of grating-patterned graphene. The combination of two distinct metals in a conductor has the potential to greatly amplify the nonlinear state of the conductor, which will lead to an increase in the specific heat capacity of the conductor. Graphene gratings connect the pump beam to two SPP waves that may cancel each other out, which results in the formation of a stationary SPP wave in the region between the gratings due to the mutual interference that occurs. The distance in between the two gratings will have its distance between them fine-tuned in order to improve the formation of second harmonics. It will be shown that field sweetening in proposed waveguides may result in significant improvements in SHG by optimizing the pure mathematics of the desired structure and using different metals. These two factors are meant to be done in conjunction with one another.

**Keywords:** SHG, MGIM, plasmonics, Graphene, grating, asymmetric structure.

**How to cite this article:** Sarani M, Khajeh zadeh A, Jafari Shabazzadeh M. (2025). A Novel Structure to Enhance Second Harmonic Generation in Plasmonic Waveguide. Management Strategies and Engineering Sciences, 7(2), 131-138.



## 1. Introduction

Plasmonic technology has seen an uptick in interest during the last several years [1-4]. There is a widespread misconception that the metal-dielectric interactions that are involved in plasmonics are quite straightforward. The electric field of the sun both accelerates and decelerates the electrons that are found on the solar surface. It's a lot like how electrons behave when they're in a plasma: very active. Because electrons are involved, the transmission of light from the sun is restricted to dimensions that are subwavelength [5]. A surface wave would be produced by collective electron oscillations that exponentially decay into two nearby [\*fr1] regions. The term "surface plasmon" refers to a synchronous electrical surface wave that resonates at the solar frequency. This mode is known as the surface plasmon (SP) mode. Although it is not possible to identify the surface-propagating wave component of the field, it does degrade exponentially into two different [\*fr1] zones.

If the electrons in these metals were accelerated, it is feasible that the rate at which sunlight gets to the surface would rise. This would be a desirable outcome. Because of this, the apparent wavelength of sunlight is likewise shortened, which makes it possible to find a field beyond the sun's limit for its optical phenomena. As a direct result of this, the size of the optical mode decreases, moving closer to the scale of subwavelengths. The distance that separates an item and a beam of light is denoted by the wavelength of the light, and the size of the beam of light is one hundred times smaller than the distance. Plasmonic waveguides are an intriguing alternative to waveguides manufactured from more typical materials because of their surface localisation.

Plasmonic waveguides with dielectric loading (DLSPPW), hybrid plasmonic waveguides, channel plasmon polaritons (CPP), and insulator-metal-insulator (IMI) waveguides are some examples of plasmonic waveguides that have been theoretically and experimentally predicted. Other types of plasmonic waveguides include hybrid plasmonic waveguides. The MGIM structure is notable for a number of reasons, including its long SPP propagation distance, its simplicity of manufacture, and its strong couplings with optical fiber and Si waveguides [6, 7]. On the other hand, it is anticipated that MGIM waveguides will be used in a range of applications, such as optical resonators [8-10], wave guide bends and splitters supported by MGIM sub-wavelength plasmonic waveguides [11-13], and resonators [14, 15]. Additionally, they are physically closer to the waveguides that surround them, which results in larger

confinement factors. There have been some investigations into surface plasmon polariton (SPP) waves that have been carried out in metal-insulator-metal hierarchical grating wave guides [16, 17].

The majority of the MGIM waveguides that have been investigated up to this point have a bilateral symmetry, which indicates that the metals located on the top and bottom of the material layer are identical. In spite of the fact that a number of investigations have been conducted to investigate the nonlinear optical processes that take place in these nonuniform waveguides, not a single one has concentrated on the MGIMs. Additionally, more research has to be done on the SHG in plasmonic waveguides since this phenomenon has received less attention up to this point. SHG is a nonlinear process that has received a significant amount of attention from researchers [18] as a result of its fascinating applications and straightforward theory. Optical devices may be made to function in the visible and ultraviolet portions of the electromagnetic spectrum by using a technique called surface holographic grating (SHG) [19]. To this day, nonlinear reactions of materials that are stable at length scales less than a wavelength are notoriously difficult to comprehend.

On the subject of SHG enhancement in plasmonic nanostructures, there is a profusion of published research to be found. Simon et al. [18] shown that the activation of surface plasmons in thin silver films resulted in a harmonic sweetening that is one and a [\*fr1] orders of magnitude more than what would be expected. This was accomplished by undertaking the first experimental and theoretical investigation of its type. Studies have also been conducted on a variety of nanowires, including those with a homogenized centro-symmetric symmetry, hybrid plasmonic waveguides, bowtie aperture arrays, and plasmonic slot waveguides [20-23].

On the other hand, SHG, which cannot be created directly in silicon, is a case where the reverse is true. The lack of second-order susceptibility in the material may be attributed to the centrosymmetry of the crystal. It is possible that the inclusion of the Si compound (Si<sub>3</sub>N<sub>4</sub>), which causes analogous second-order nonlinear processes in structures that are compatible with Si [24-26], would assist to mitigate the effects of this constraint. Recently, Oliveira et al. [26] employed the electric-field-induced SHG technique to manufacture SHG in a Si<sub>3</sub>N<sub>4</sub> ring resonator with a diameter of 20 meters. They were able to achieve a conversion potency of around  $3.68 \times 10^3$  at a pumping power of 75 mw. The employment of plasmonic-based nonlinear devices,

namely those employing the LiNbO<sub>3</sub> crystal, which provides strong local enhanced confinement of light beyond the restrictions necessitated by the laws of optical processes in material media [27], is one of the greatest possibilities for attaining this ambition. There have been several discoveries made about the many forms of projected plasmonic structures. The price of SHG has been brought down for a variety of different materials, such as plasmonic slot waveguides (PSW) [19], long-range plasmonic waveguides (38), hybrid plasmonic waveguides (39), nano-scale roughness on metal surfaces [28], individual aluminiferous nano-aperture [29], plasmonic particle chains [28], and plasmonic core-shell nanowires [30]. [19]; [31]; [29];

Lithium niobate is a common component found in optoelectronics and other electrical devices. It is still used in a wide variety of devices, such as surface acoustic wave (SAW) filters and modulators in the field of physics, as well as electro-optic modulators, q-switches, and frequency conversion in the field of optics. Because of its exceptional electrical, electro-optical, and nonlinear optical properties, niobate makes for an excellent material platform. In recent years, niobate's (a metallic element with nonlinear optical characteristics) use as a material for optical frequency conversion has expanded significantly. Niobate is a nonlinear optical material. Niobate is an element that is composed of metal, and it has very high quadratic susceptibilities. This demonstrates that, particularly at optically high powers, a significant amount of polarization is generated inside the crystal, and that this polarization is proportional to the product of two incoming field components [17, 32]. Furthermore, this polarization is proportional to the fact that there is a significant amount of polarization generated inside the crystal at optically high powers. According to the findings of our study, metallic element minerals are the nonlinear material that is employed in such systems for comprehending SHG [18] the majority of the time. Even though the typical CW pump power of the fundamental frequency (FF) is only approximately one watt, it is customary practice to set a maximum power limit of 105 watts for the height powers of the ensuing second harmonic frequency (SHF) [19]. Even if the power is increased to 102 W in HPW, it is probable that the corresponding wave path length of one millimeter [33] will be too lengthy for future nano-photonics integrated circuits. This is the case even if the power is increased. Because of the comparatively low nonlinear susceptibility in crystal, the relatively large nonlinear coupling coefficients across entirely independent

frequencies, and the absorption loss of the plasmonic modes, the purported efficiency is unusually poor.

This is the first work to investigate SHG in non-ideal plasmonic waveguides, which we provide here. The problem of low nonlinear susceptibility can be solved by employing two "different" metals that have enormous nonlinear coupling coefficients between different frequencies. Additionally, the problem of the absorption loss of the plasmonic modes can be circumvented by using two gratings that are identical to one another. By making adjustments to the spacing distance and the length of the two gratings, it was possible to improve the part-matching condition and significantly increase the SHF. Gold and silver are the two types of metals that are used in the construction of the MGIM plasmonic wave guide. After utilizing solely mathematical approaches to optimize the grating, the results showed that it had an unbalanced structure (Gold-LiNbO<sub>3</sub>-Silver) that had a greater SHG than conventional structures. The resultant frequency of the second harmonic is then given an additional height power of zero. At the 44 W. location, there are plans to build a GRATING GRAPHENE structure. When evaluating the proposed building in comparison to other, more traditional constructions, the pump power of the FF, which is 1 W, is taken into consideration. For the sake of this undertaking, the commercial finite element program COMSOL was used for all of the simulation calculations.

In order to make the organization of this post a little easier to grasp, allow me to first explain: The structure of the predicted wave guidance is often detailed in Section 2, as is the case here. The final section presents the numerical findings obtained by SHG while operating inside the specified framework.

## 2. The Structure of MGIM Maveguide

The construction of the grating graphene MIM plasmonic waveguide is seen in Figure 1. In this structure, between the top and bottom metals lies a 50 nm layer of lithium niobite. The top metal layer has two identical gratings. In this configuration, the top and bottom metals are distinct. Both metals' thicknesses (H) are set at 100 nm and considered constants. The starting determinations for the period and depth of the dents are 50 nm and 70 nm, respectively, and the right and left gratings are identical. Remember that the tooth depth has a substantial effect on coupling efficiency.

Deeper teeth result in increased productivity. In this instance, however, we do not consider coupling efficiency at its apex. In addition to coupling the pumped light into the MIM waveguide, the grating also couples a portion of the light outside the waveguide. In order to achieve a balance between these two lights, the coupling efficiency must be taken into account, and the notch depth must be changed to provide the best SHG efficiency. The calculation for the duty cycle is  $d_1/d_2$ . This duty cycle has been tuned to provide the highest SHG efficiency and peak power. After assuming that the distance between the two gratings is 1500 nm, the location and power of the resulting SHF peak are calculated. This distance is then optimized for optimal performance. The length of the waveguide is predicted to be 2.5  $\mu\text{m}$ . As a result, the right and left sides each contain exactly 10 teeth. The picture also depicts two square-shaped air openings on either side of the building.

As shown in Figure 1, a strong pump and a weak signal are used to examine the photorefractive impact of the suggested structure. Asymmetric plasmonic waveguides support two distinct modes [5, 15-18]. Literature differentiates between symmetric and anti-symmetric modes, long range surface plasmon polariton (LRSPP) and short range surface plasmon polariton (SRSPP), and even and odd modes [15-19]. A quasi-symmetric and quasi-antisymmetric mode may exist in an asymmetric plasmonic waveguide [15-18, 33]. As with symmetric waveguides, its designation is based on the charge distribution over the central layer. Figure 2 illustrates the profile diagrams for each mode. Figure 2 (b) represents the profile of quasi-

symmetric and quasi-anti-symmetric modes for an asymmetric MIM plasmonic device, while Figure 2 (c) depicts the profile of quasi-symmetric and quasi-antisymmetric modes for the proposed structure. Figure 2 depicts the profile of symmetric and asymmetric modes for a symmetric MIM plasmonic waveguide (a). Observably, the spherical profiles are bent asymmetrically. As a result, asymmetric structures exhibit a unique quasi-symmetric and quasi-antisymmetric mode profile compared to symmetric structures. In this article, the terms "symmetric" and "asymmetric" modes are used to represent both symmetric and asymmetric structures. The pairing of the two SPP modes is caused by the photorefractive effect. In the presence of a strong symmetric mode, a weak asymmetric mode may acquire sufficient energy up to a certain waveguide length. It will be demonstrated that the suggested designs generate higher advantages and that the gains can be sustained across a wider range of waveguide lengths. The essential geometrical features of the suggested structure, such as grating duration and spacing, are also explored in terms of how they effect photorefractive gain.

In this research, the wavelength of operation of  $\lambda=458$  nm was considered. At this wavelength, the permittivity of crystal is  $\epsilon_z=5.1772$  and  $\epsilon_x=5.6243$ , the permittivity of Aluminum is  $\epsilon_{Al}=-29 + 7i$ , the permittivity of Gold is  $\epsilon_{Au}=-1.3 + 4.6i$ , and the permittivity of Silver is  $\epsilon_{Ag}=-6 + 0.66i$ . All the simulations in this paper were performed by using rigorous numerical schemes based on the finite-element method (FEM).

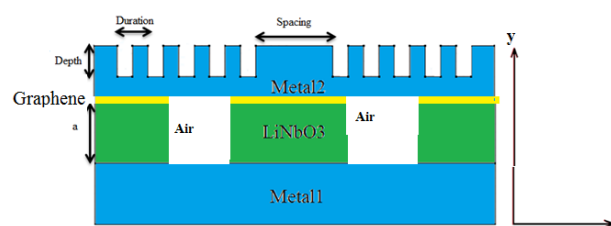


**Figure 1.** Structure of the proposed GRATING GRAPHENE MGIM waveguide under consideration

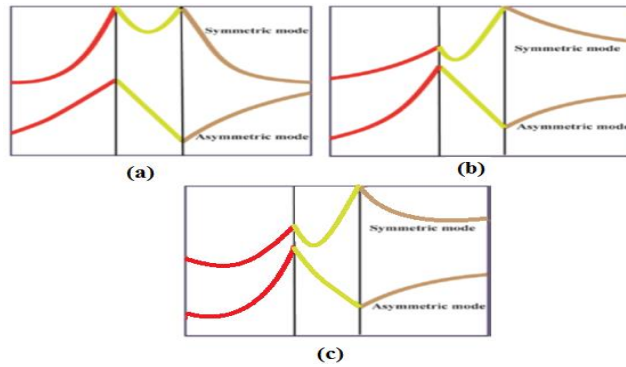
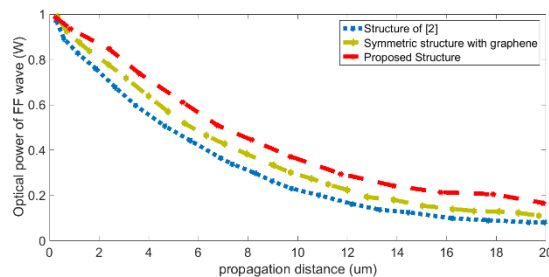


**Figure 2.** Schematic diagram of symmetric and asymmetric modes in (a) symmetric structure, (b) asymmetric structure [2], (c) Proposed structure.

### 3. Results and Discussion

The results of simulations run on many different plasmonic waveguides are presented here for your perusal. In [1], it was shown beyond a reasonable doubt that an asymmetrical Au-LiNbO<sub>3</sub>-Ag combination had the potential to produce a sizeable second harmonic wave. In the next section, we will demonstrate how the GRATING GRAPHENE Structure has the potential to significantly improve the nonlinear optical process of creating second harmonics. The structure that is being presented is quite similar to those that are described in [1, 2] with the exception that it makes use of graphene and improves upon its features. A model of a symmetric graphene structure is used here to help put this into perspective. In Figure 2, the optical intensities of FF (top) and SHF (bottom) waves are displayed for three distinct structures as a function of the distance that the waves have traveled since they were generated. As can be seen from the image, the SHF optical power as well as the FF wave distance are both increased to their full potential in the asymmetric design. The inherent imbalance that exists

between the two modes is amplified as a result of the graphene layer's introduction of new modifications to the space charge electric field. It is believed that this imbalance contributes to an increase in nonlinear susceptibility as well as the SHG process. In addition, the FF optical power in the suggested structure is equivalent to that observed in the structure of [1], even at a distance of 20  $\mu\text{m}$ , as a consequence of the decreased propagation attenuation. This was found to be the case due to the fact that the suggested structure attenuates light less than the structure of [1]. At a height of 2  $\mu\text{m}$ , 0.35 W of SHF optical power is the greatest height that can be found. For the sake of this scenario, the optimal normalized conversion efficiency is determined to be  $2.22 \times 10^7 \text{ W}^{-1} \text{ cm}^{-2}$ . This is about eight times greater than the finding from [2] and approximately five times higher than the finding from [2] for LiNbO<sub>3</sub>-based PSW devices. According to these findings, the suggested structure is superior to both the symmetric and the asymmetrical alternatives in terms of SHF optical power, and it also has a peak position that is more ideal. In actual use, this structure exhibits a lower attenuation of propagation while simultaneously exhibiting a greater nonlinear susceptibility.



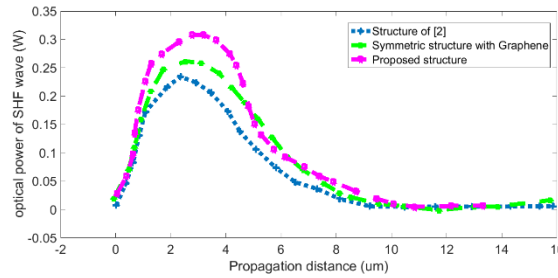


**Figure 3.** The optical powers of FF (top) and SHF (bottom) waves as a function of propagation distance and for different structures

Figure 3 illustrates the frequency spectra as well as the Ey distributions of two different structures. As can be seen in the graphic, the proposed construction has a much higher

peak electric field strength than the alternative. Graphene is another factor that leads to the shift in the frequency of SHG.

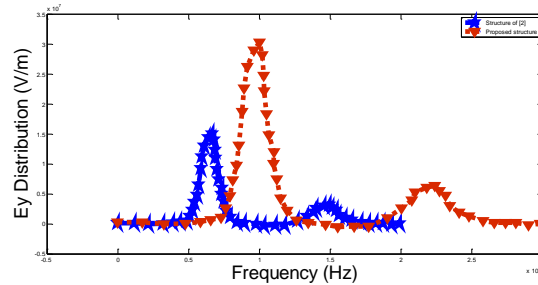


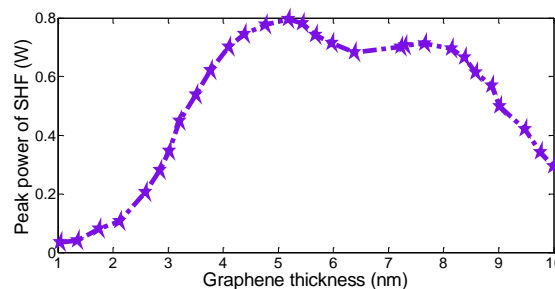
**Figure 4.** Ey distribution of different structures.

The inclusion of graphene has resulted in a significant increase in the peak electric field experienced by the structure, as can be seen in the accompanying picture. As a result of the enhancement in the electric field, which promotes SHG amplification and can be observed as an increase in the second harmonic component, a second harmonic wave with a frequency of 11015 Hz is formed as a consequence of the change.

crystal thickness at which the electric field is at its most intense. The phase-matching condition would change depending on the thickness of the graphene, which might have a substantial effect on the superconducting hybrid field. It is possible to correctly determine the thickness of graphene at which the phase match criteria is considered to be met. If we assume this thickness of graphene, we attain the maximum magnitude of the second harmonic surface electric field.

The second harmonic surface electric field was shown to have a variable relationship with the amplitude of motion of the graphene sheet. The second harmonic surface electric field is shown plotted against the thickness of the graphene in Figure 5. The diagram demonstrates that there is a certain

This graph suggests that the SHF should run at a maximum power of 0.8 watts and should be positioned in the ideal position of 0.5. (um).



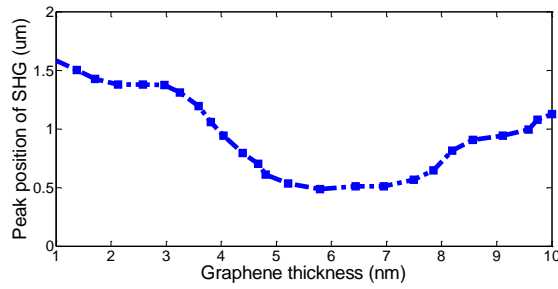


**Figure 5.** The peak optical power of SHF and peak position of the SHG process as a function of the Graphene layer.

Figure 6 shows the frequency spectra as well as the EY distributions of the suggested structure that was optimized. Compare this figure with Figure 3 to get an idea of how

much the peak electric field of the optimally advised structure has been improved.

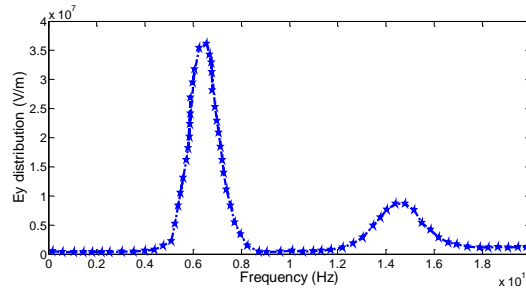


**Figure 6.** Ey distributions and frequency spectra of optimized proposed structure

**4. Conclusion**

This study presents a novel asymmetric construction that consists of two separate metals, two identical gratings, and a thin layer of graphene. The goal of this design is to improve the optical power of SHF while simultaneously decreasing its peak position. The symmetric and asymmetric Metal-Graphene-insulator-Metal plasmonic waveguides were analyzed by the researchers to see how the SHG behaved in each configuration. In this particular instance, a block of lithium niobite was used to construct an insulator. It was shown that the proposed plasmonic waveguide has the capability of generating a significant second harmonic wave. The recommended layout's SHF peak optical power was 0.8 W, which is an improvement over earlier structures; also, the suggested layout's peak position was 0.5 um. As a consequence of this, the plasmonic waveguide that was presented is a structure that is functional for conceivable SHG uses in the future.

**Authors' Contributions**

Authors equally contributed to this article.

**Acknowledgments**

Authors thank all participants who participate in this study.

**Declaration of Interest**

The authors report no conflict of interest.

**Funding**

According to the authors, this article has no financial support.

**Ethical Considerations**

All procedures performed in this study were under the ethical standards.

**References**

- [1] S. Abdollahramezani *et al.*, "Tunable nanophotonics enabled by chalcogenide phase-change materials," *Nanophotonics*, vol. 9, pp. 1189-1241, 2020, doi: 10.1515/nanoph-2020-0039.
- [2] S. Abdollahramezani *et al.*, "Dynamic hybrid metasurfaces," *Nano Lett.*, vol. 21, pp. 1238-1245, 2021, doi: 10.1021/acs.nanolett.0c03625.
- [3] A. Ahmadvand and B. Gerislioglu, "Deep- and vacuum-ultraviolet metaphotonic light sources," *Mater. Today*, vol. 51, pp. 208-221, 2021, doi: 10.1016/j.mattod.2021.05.019.
- [4] J. Zhang, E. Cassan, D. Gao, and X. Zhang, "Highly efficient phase-matched second harmonic generation using an asymmetric plasmonic slot waveguide configuration in hybrid polymer-silicon photonics," *Opt. Express*, vol. 21, 2013, doi: 10.1364/OE.21.014876.
- [5] S. A. Maier, *Plasmonics, Fundamentals and Applications*. Springer, 2007.
- [6] R. X. Yang, R. A. Wahsheh, Z. L. Lu, and M. A. G. Abushagur, "Efficient light coupling between dielectric slot waveguide and plasmonic slot waveguide," *Opt. Lett.*, vol. 35, pp. 649-651, 2010, doi: 10.1364/OL.35.000649.
- [7] P. Neutens, P. Van Dorpe, I. De Vlaminck, L. Lagae, and G. Borghs, "Electrical detection of confined gap plasmons in Metal-Graphene-insulator-Metal waveguides," *Nat. Photonics*, vol. 3, pp. 283-286, 2009, doi: 10.1038/nphoton.2009.47.
- [8] K. Wen *et al.*, "Multiple Plasmon-Induced Transparency Responses in a Subwavelength Inclined Ring Resonators System," *IEEE Photonics Journal*, vol. 7, no. 6, pp. 1-7, 2015, doi: 10.1109/JPHOT.2015.2504966.
- [9] K. Wen, Y. Hu, L. Chen, J. Zhou, L. Lei, and Z. Guo, "Fano resonance with ultra-high figure of merits based on plasmonic Metal-Graphene-insulator-Metal waveguide," *Plasmonics*, vol. 10, no. 1, pp. 27-32, 2015, doi: 10.1007/s11468-014-9772-6.
- [10] K. Wen, Y. Hu, L. Chen, J. Zhou, L. Lei, and Z. Meng, "Single/dual Fano resonance based on plasmonic metal-dielectric-metal waveguide," *Plasmonics*, vol. 11, no. 1, pp. 315-321, 2016, doi: 10.1007/s11468-015-0056-6.
- [11] H. T. Miyazaki and Y. Kurokawa, "Squeezing visible light waves into a 3-nm-thick and 55-nm-long plasmon cavity," *Physical Review Letters*, vol. 96, p. 097401, 2006, doi: 10.1103/PhysRevLett.96.097401.
- [12] G. Veronis and S. Fan, "Bends and splitters in metal-dielectric-metal subwavelength plasmonic waveguides," *Applied Physics Letters*, vol. 87, p. 131102, 2005, doi: 10.1063/1.2056594.
- [13] Y. Kurokawa and H. T. Miyazaki, "Metal-Graphene-insulator-Metal plasmon nanocavities: Analysis of optical properties," *Physical Review B*, vol. 75, p. 035411, 2007, doi: 10.1103/PhysRevB.75.035411.
- [14] Y. Xie *et al.*, "Theoretical investigation of a plasmonic sensor based on a metal-insulator-metal waveguide with a side-coupled nanodisk resonator," *Journal of Nanophotonics*, vol. 9, no. 1, 2015, doi: 10.1117/1.JNP.9.093099.
- [15] Y. Xie, Y. Huang, and W. Zhao, "A Novel Plasmonic Sensor Based on Metal-Insulator-Metal Waveguide With Side-Coupled Hexagonal Cavity," *IEEE Photonics Journal*, vol. 7, no. 2, 2015, doi: 10.1109/JPHOT.2015.2419635.
- [16] C. Zeng and Y. Cui, "Rainbow trapping of surface plasmon polariton waves in metal-insulator-metal graded grating waveguide," *Optics Communications*, vol. 290, pp. 188-191, 2013, doi: 10.1016/j.optcom.2012.10.020.
- [17] C. Zeng and Y. Cui, "Low-distortion plasmonic slow-light system at telecommunication regime," *Optics Communications*, vol. 294, pp. 372-376, 2013, doi: 10.1016/j.optcom.2012.12.037.
- [18] R. W. Boyd, *Nonlinear Optics*. Academic, 2008.
- [19] T. Harimoto, B. Yo, and K. Uchida, "A novel multipass scheme for enhancement of second harmonic generation," *Opt. Express*, vol. 19, 2011, doi: 10.1364/OE.19.022692.
- [20] C. G. Biris and N. C. Panoiu, "Second harmonic generation in metamaterials based on homogeneous centrosymmetric nanowires," *Phys. Rev. B*, vol. 81, no. 19, 2010, doi: 10.1103/PhysRevB.81.195102.
- [21] F. F. Lu, T. Li, X. P. Hu, Q. Q. Cheng, S. N. Zhu, and Y. Y. Zhu, "Efficient second harmonic generation in nonlinear plasmonic waveguide," *Opt. Lett.*, vol. 36, 2011, doi: 10.1364/OL.36.003371.
- [22] S. Park, J. W. Hahn, and J. Y. Lee, "Doubly resonant metallic nanostructure for high conversion efficiency of second harmonic generation," *Opt. Express*, vol. 20, 2012, doi: 10.1364/OE.20.004856.
- [23] C. C. Neacsu, G. A. Reider, and M. B. Raschke, "Second harmonic generation from nanoscopic metal tips: symmetry selection rules for single asymmetric nanostructures," *Phys. Rev. B*, vol. 71, 2005, doi: 10.1103/PhysRevB.71.201402.
- [24] M. Cazzanelli *et al.*, "Second-harmonic generation in silicon waveguides strained by silicon nitride," *Nat. Mater.*, vol. 11, no. 2, pp. 148-154, 2011, doi: 10.1038/nmat3200.
- [25] J. S. Levy, M. A. Foster, A. L. Gaeta, and M. Lipson, "Harmonic generation in silicon nitride ring resonators," *Opt. Express*, vol. 19, no. 12, pp. 11415-11421, 2011, doi: 10.1364/OE.19.011415.
- [26] R. E. P. de Oliveira, M. Lipson, and C. J. S. de Matos, "Electrically controlled silicon nitride ring resonator for quasi-phase matched second-harmonic generation," in *in CLEO: Science and Innovations*, 2012: Optical Society of America, doi: 10.1364/CLEO\_SI.2012.CF3M.5.
- [27] M. L. Brongersma and P. G. Kik, *Surface Plasmon Nanophotonics*. Springer, 2007.
- [28] A. R. Davoyan, I. V. Shadrivov, and Y. S. Kivshar, "Quadratic phase matching in nonlinear plasmonic nanoscale waveguides," *Opt. Express*, vol. 17, no. 22, pp. 20063-20068, 2009, doi: 10.1364/OE.17.020063.
- [29] W. S. Cai, A. P. Vasudev, and M. L. Brongersma, "Electrically controlled nonlinear generation of light with plasmonics," *Science*, vol. 333, no. 6050, pp. 1720-1723, 2011, doi: 10.1126/science.1207858.
- [30] S. B. Hasan, C. Rockstuhl, T. Pertsch, and F. Lederer, "Second-order nonlinear frequency conversion processes in plasmonic slot waveguides," *J. Opt. Soc. Am. B*, vol. 29, no. 7, pp. 1606-1611, 2012, doi: 10.1364/JOSAB.29.001606.
- [31] M. I. Stockman, "Nanoplasmonics: past, present, and glimpse into future," *Opt. Express*, vol. 19, no. 22, pp. 22029-22106, 2011, doi: 10.1364/OE.19.022029.
- [32] A. Yariv, "Phase conjugate optics and real-time holography," *IEEE Journal of Quantum Electronics*, vol. 14, no. 9, pp. 650-660, 1978, doi: 10.1109/JQE.1978.1069870.
- [33] H. J. Simon, D. E. Mitchell, and J. G. Watson, "Optical second harmonic generation with surface plasmons in silver films," *Phys. Rev. Lett.*, vol. 33, 1974, doi: 10.1103/PhysRevLett.33.1531.